

# Mitigating inefficient task mappings with an Adaptive Resource-Moldable Scheduler (ARMS)

Mustafa Abuljabbar  
Chalmers University of Technology  
Gothenburg, Sweden  
musabdu@chalmers.se

Mahmoud Eljammaly  
Gothenburg, Sweden  
jammaly@iee.org

Miquel Pericàs  
Chalmers University of Technology  
Gothenburg, Sweden  
miquelp@chalmers.se

## ABSTRACT

Efficient runtime task scheduling on complex memory hierarchy becomes increasingly important as modern and future High-Performance Computing (HPC) systems are progressively composed of multi-socket and multi-chiplet nodes with nonuniform memory access latencies. Existing locality-aware scheduling schemes either require control of the data placement policy for memory-bound tasks or maximize locality for all classes of computations, resulting in a loss of potential performance. While such approaches are viable, an adaptive scheduling strategy is preferred to enhance locality and resource sharing efficiency using a portable programming scheme. In this paper, we propose the Adaptive Resource-Moldable Scheduler (ARMS) that dynamically maps a task at runtime to a partition spanning one or more threads, based on the task and DAG requirements. The scheduler builds an online platform-independent model for the local and non-local scheduling costs for each tuple consisting of task type (function) and task topology (task location within DAG). We evaluate ARMS using task-parallel versions of SparseLU, 2D Stencil, FMM and MatMul as examples. Compared to previous approaches, ARMS achieves up to 3.5X performance gain over state-of-the-art locality-aware scheduling schemes.

## KEYWORDS

Parallel Runtime Scheduling, DAG Applications, Locality-Aware Scheduling, Adaptive Scheduling, Performance Portability

### ACM Reference Format:

Mustafa Abuljabbar, Mahmoud Eljammaly, and Miquel Pericàs. 2021. Mitigating inefficient task mappings with an Adaptive Resource-Moldable Scheduler (ARMS). In *Proceedings of ACM Conference (Conference'17)*. ACM, New York, NY, USA, 13 pages. <https://doi.org/10.1145/nnnnnnn.nnnnnnn>

## 1 INTRODUCTION

The trend towards larger many/multicore architectures adds pressure on the memory technology in order to sustain maximum performance. Such advancements typically target reducing latency, increasing and scaling data transfer bandwidth. For a parallel program running on such platforms, performance is often subject to data access latency that varies based on where the data resides. This may

range from local resources (e.g. L1/L2 caches) to uncore resources such as the L3 or DRAM. Furthermore, to increase the DRAM bandwidth and capacity, computing nodes increasingly leverage within-socket [32, 37] and multi-socket [12, 31] Non-Uniform Memory Access domains (NUMA) partitions, adding yet another level to the memory hierarchy. This makes the optimization of parallel programs rather more challenging as it is potentially impacted by nonuniform data access latency, memory channel bandwidth and resource contention. These challenges are often addressed by approaches that have the goal of maximizing data locality [43]. Thus, advanced programming, runtime and compiler level techniques have been introduced to handle the resulting asymmetry in access speeds, to overcome penalties of non-local requests and maximize the utilized bandwidth [4, 13, 30, 43].

One of the expressive parallel programming paradigms are the task-based programming models [20, 33, 45, 46]. These are frequently used to express the parallelism of the program in the form of tasks. The task scheduling problem (i.e. mapping tasks to execution units such as threads) is, however, nontrivial. This is particularly true with the growing complexity of task DAGs (Direct Acyclic Graph) and execution platforms. Therefore, scheduling must be performed online by the task-based runtime schedulers.

Many schedulers embraced by modern task-parallel runtime libraries leverage random work-stealing as it achieves dynamic load-balance and increases the average core utilization [8]. Hence, work-stealing has become the de facto implementation choice of many task-parallel runtime systems. Nonetheless, random work-stealing assumes a flat view of the memory resources and is bound to suffer a considerable performance penalty, especially when scheduling tasks whose performance is influenced by data access latency and bandwidth.

For this reason, locality-aware extensions to work stealing have been proposed to mitigate the effects of non-local memory/cache access latency. These schedulers fall into three categories. In the first category, the task-DAG's input/output dependencies are analyzed to devise a locality-aware schedule [18, 19, 36]. Tasks are then mapped to reduce a distance metric based on a static description of the hardware topology, which explains how the different hardware components (such as caches, memory controllers, cores, threads, etc.) are organized. A second category focuses on creating work-stealing regions with low latency memory access. This is achieved by leveraging locality hints from the programmer to aggregate the tasks into execution places (i.e. collections of cores) that can be configured to match the hardware architecture such as threads, cores or sockets. Examples of this approach include LAWS [24], ADWS [38], SWAS [42] and Olivier et al. [34]. In the third category, the task data allocation is controlled by the runtime to evenly

Permission to make digital or hard copies of all or part of this work for personal or classroom use is granted without fee provided that copies are not made or distributed for profit or commercial advantage and that copies bear this notice and the full citation on the first page. Copyrights for components of this work owned by others than ACM must be honored. Abstracting with credit is permitted. To copy otherwise, or republish, to post on servers or to redistribute to lists, requires prior specific permission and/or a fee. Request permissions from [permissions@acm.org](mailto:permissions@acm.org).

Conference'17, July 2017, Washington, DC, USA

© 2021 Association for Computing Machinery.

ACM ISBN 978-x-xxxx-xxxx-x/YY/MM... \$15.00

<https://doi.org/10.1145/nnnnnnn.nnnnnnn>

distribute the data over the available NUMA domains, then schedule tasks close to their known data regions [15].

While locality-driven execution is a key factor to reducing data access latency and increasing performance, the overall application performance gain is subject to elements that are not clearly addressed by such schemes. Consider, for example, the arithmetic intensity (AI, i.e. flops per byte ratio). Application kernels with high AI are less impacted by data placement and can benefit from maximizing the compute throughput of all available execution units. This can be achieved by using simple greedy schemes such as work stealing. Hence, such applications do not benefit from the scheduling schemes that start by by maximizing locality and then applying work stealing [38], or schemes that limit their scope to tasks that have higher LLC miss rates [19]. Another key element to achieving higher application performance is maximizing the task data reuse and reducing resource requirements (e.g. bandwidth). This is specifically important for fine-grain task whose data size is within the lower level caches. Finally, it is not clear how such schedulers behave in events of lower DAG parallelism, which can be a result of unwinding the recursion in common divide-and-conquer DAGs that are a special case of fully strict DAGs [8]. In light of these elements, a scheduler that dynamically adapts to the task and DAG requirements (e.g. flops, channel bandwidth, cache reuse, parallelism, criticality) can obtain high performance on a variety of platforms while at the same time simplifying the programmer's task.

This paper proposes ARMS, the Adaptive Resource-Moldable Scheduler. ARMS dynamically builds a model of the performance of each application task on the system resource partitions, such as the cores that share cache levels, NUMA nodes, sockets, etc. The model used, herein, serves as a predictor for the performance of a task on the available system resource partitions, and guides the scheduling decisions. It is created at runtime for each task based on its location in the task DAG topology. Software topology information is used as a portable key by the runtime to map the logical location of task's input (e.g. the Cartesian coordinates or the matrix indices) to a physical core. In the absence of topology information, the scheduler automatically assigns a relative address to the task based on its location in the DAG (depth and breadth). Hence, ARMS is able to model the effects of scheduling a task on multicore partitions within or outside of its data region (e.g., NUMA node), identified by the task's specific topology location. Then, it uses this knowledge to create a schedule that reduces the per-task parallel cost. In addition, ARMS supports not only traditional 1:1 mapping (i.e. a single task to a single thread) but also 1:M mapping (i.e. moldability when 1 task is assigned M resources via worksharing). A moldable task encompasses an internal scheduler that assigns the work partitions to threads within the task function. This, in essence, represents a Single-Program-Multiple-Data (SPMD) region. The flexibility in the mapping allows, for example, a memory-bound task to leverage a higher memory bandwidth by using more resources (threads), while a resource intensive task can set the number of threads to match its cache requirements. Also, the number of threads assigned to a task is dynamically changed based on the DAG's parallelism.

The main contributions of this work are as follows:

**Listing 1: 1D N-Body task (for 1-unit mass bodies).**

```

1 void n_body(pos_target[in/out], pos_source[in], time_step, size) {
2   // set partition start and end
3   [start, end] = get_partition(_tid, _resource_width, size);
4   for(i = start; i < end; ++i) {
5     Fx = 0
6     for(j = 0; j < size; ++j) {
7       dx = pos_target[i] - pos_source[j];
8       invDist = rsqrt(dx * dx + SOFTENING)
9       Fx += dx * invDist
10    }
11    pos_target[i] += // use Fx and timestep to update position
12  }
13 }

```

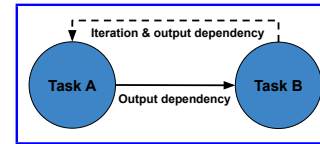


**Figure 1: Motivational N-Body DAG.**

- We identify the key parameters that constitute a locality adaptive performance model for a task, which are the task work function and the topology information.
- We map the parameters to a model that captures the performance on the available execution places, which is used by ARMS via a novel resource selection algorithm to deliver schedules that achieve good balance between locality and parallelism.
- We conduct a thorough analysis of the effectiveness of ARMS against the state-of-the-art schedulers. This study reveals that even where there is a high DAG concurrency, resource aggregation (i.e. with 1:M mapping) is inevitable for memory intensive tasks, and in events of changing DAG parallelism. It also demonstrates that for tasks with high-compute intensity, locality maximizing schedules should be avoided.

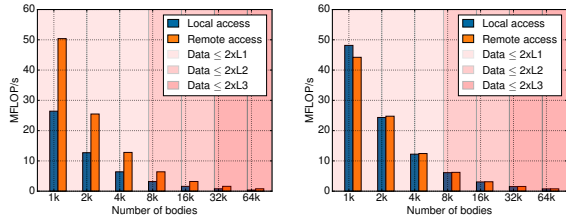
The rest of the paper is organized as follows: Section 2 introduces the scope and a few useful scheduling terminology used in this paper. Section 3 describes the scheduling algorithm and the components used to develop the dynamic locality scheduling decisions. In Section 4, we describe the evaluated applications and the experimental methodology. Finally, Section 5 evaluates the scheduler with respect to locality-aware and traditional techniques. Section 6 highlights the related work in the field of locality-aware work-stealing runtimes. Finally, Section 7 concludes the paper.

## 1.1 Motivation

Figure 2 shows the impact of data locality and task work size on the core performance using a compute-intensive chain of N-Body tasks running on a dual-socket 16-core Intel Skylake (described in Section 4). The study compares single-threaded (non-moldable) to dual-threaded tasks (a molding option). The experimental DAG chain is shown by Figure 1, where the dotted line represents both an iteration and an output dependency from Task B back to Task A. Caches are flushed after each iteration to analyze the effect of streaming data across local and remote NUMA domains. The cache reuse happens within the iteration. Then, the chain is terminated

**Table 1: Task computation and data locations for motivational DAG (Figure 1) discussed by Figure 2. The table shows the configurations for the moldable and non-moldable cases for the local and remote scenarios.**

Scenario	Mode	Not molded		Molded	
		Task A	Task B	Task A	Task B
Local access	Task				
	Execution thread id(s)	0	0	0, 1	0, 1
	NUMA node id for data	0	0	0	0
Remote access	Execution thread id(s)	0	16	0, 1	16, 17
	NUMA node id for data	0	1	0	1



(a) Core MFLOP/s for a direct N-Body DAG chain when tasks are **not molded** (i.e. single-threaded) (b) Core MFLOP/s for a direct N-Body DAG chain when tasks are **molded** to two threads

**Figure 2: Discussing the dynamic factors that impact the core performance which include task size, data location, and task molding (averaging 30 runs) on a dual-socket Intel Skylake.**

after 1000 iterations to get a sustainable flops rate. Performance is expressed using the core flops (MFLOP/s). The average is taken across multiple runs to give a statistical guarantee over reproducibility. The shaded regions in Figure 2 depict the different levels of the caches where the total working set fits. Listing 1 briefly highlights the benchmark evaluated herein. It shows a direct N-Body ( $N^2$ ) computations using 2 threads. The output of task A is input to task B and so on. The start and end indices mark the partition that the task works on in case of moldable execution. The task’s data pointer (i.e. `pos_target`) is either pinned to the local NUMA or remote NUMA. Specification of computation and data locations are shown in Table 1. The “not molded” column shows the configurations used for Figure 2(a), whereas the “molded” column shows the configurations used for Figure 2(b). So for the chain of executions of task A followed by task B, we specify the computation thread id, and the NUMA id of the cell data (the N-Body domains are usually structured as trees). In this case, the cell data is `pos_target` as per Listing 1. For example, in the “Remote access” scenario, the `pos_target` output of task B located on NUMA node 1 would be `pos_source` input to task A that executes on a thread 0 residing on remote NUMA node 0.

We make two observations here: First, if we consider the “molded” case shown by Figure 2(b), NUMA-aware computation (i.e. Local access) for this benchmark is beneficial only for the finest grain case (input size = 1k). Second, when the task is not molded (as shown in Figure 2(a)), there is no gain in preserving NUMA locality. Interestingly, in the absence of moldability, the most locality preserving approach, that is running dependent tasks on thread 0

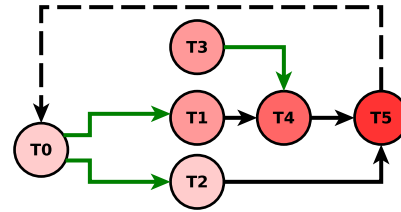


**Figure 3: Sample generic DAG discussed in this paper. Green line indicates execution dependencies. Black line indicates data dependencies. Dotted line is an iteration (not a cycle).**

and allocating on the local NUMA node, does not perform well on average, as shown by the blue bars in Figure 2(a). This is the case when computation is done next to the data in physical memory using a single thread to maximize L1 cache reuse. So, in practice such a choice incurs an evident performance degradation in certain cases. In this case, “remote” wins because of the interleaved access to multiple memory channels (0,1) from tasks A and B when data is distributed over 2 memory domains. As these observations vary based on the application, they make dynamic task scheduling decisions even more desirable, since the best mapping depends on the underlying platform, class of computation, and granularity of task among other attributes. The main hypothesis behind ARMS is that the impact of scheduling decisions can be estimated via an online performance model that is aware of the task type and of topology information that encodes the data location.

## 2 SCOPE AND BACKGROUND

This work targets a general form of DAGs with iterative or recursive structure, where nodes represent tasks and edges are either execution or data dependencies as shown by the synthetic example in Figure 3. The black edges refer to direct data dependencies (i.e. there is an edge from  $T_a$  to  $T_b \iff T_b$  directly reuses output data from  $T_a$ ). The green edges refer to execution dependencies (i.e. there is an edge from  $T_a$  to  $T_b \iff T_b$  cannot start unless  $T_a$  has completed execution). For example, a task-based version of post-order recursive traversal would not visit a node unless all descendants have been traversed. The dotted line indicates an iteration, which is a concatenation of the DAG to itself for an  $X$  number of iterations. This edge does not indicate a cycle as the execution terminates after the program iterations have elapsed. The gradient change in red color indicates a different task type. A task type in the context of this work represents the task’s work function. Figure 4 depicts the possible Resource Partitions ( $R_p$ ) denoted by the Leader ( $LR$ ) logical thread id, which is the thread with the smallest id in the partition, and the Width ( $W$ ) of the partition, which is the number of workers (i.e. logical threads) involved.  $T_a$  can be mapped to a work-sharing region with  $W >= 1 \iff T_a$  is moldable.

## 3 ADAPTIVE RESOURCE-MOLDABLE SCHEDULER (ARMS)

In a parallel system, if the available resource partitions are denoted by  $R_p = \{R_0, R_1, \dots, R_{p-1}\} : R_i = [LR, W]$ , then each invocation of

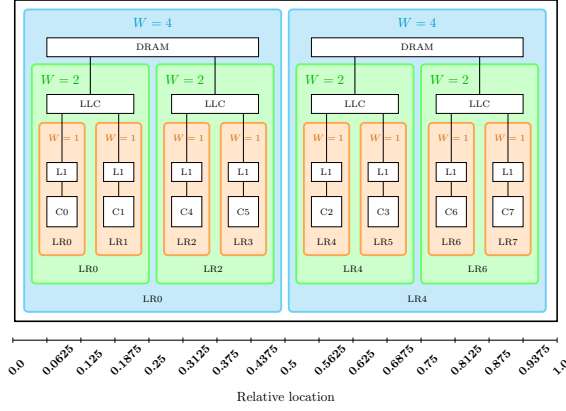


**Figure 4: An example mapping of relative topological locations. For instance, 0.125 maps to an initial worker id of 1 ( $0.125 \times 8$ ). This worker falls in execution places:  $R_0 = [LR = 0, W = 1]$ ,  $R_1 = [LR = 0, W = 2]$  and  $R_2 = [LR = 0, W = 4]$ .**

ARMS (denoted by  $S$ ) on a task  $\tau$  should return  $R_x$  ( $S(\tau) = R_x \in R_p$ ). Therefore, this section describes the different components of ARMS. In Section 3.1, we define the concept of STA (Software Topology Address) and show how to construct STAs in order to differentiate between the performance models based on locality. Then in Section 3.2, we show how we build the moldable resource partitions that are to be analyzed by the model. Section 3.3 highlights the resource selection algorithm. These components are necessary to determine what constitutes an efficient resource partition to schedule a specific task based on an online performance model.

### 3.1 The Software Topology Address Construction

Among the common techniques in constructing logical representations of spatial domains is using graph, geometric or algebraic forms. For example, continuous air particles, once discretized, can be expressed as mesh topology points accessed by their Cartesian coordinates. This matrix-free representation is useful for carrying out stencil updates. Since the topology is a static description of the domain, we propose to use it to create a portable initial mapping of the location of task’s data to a physical location in hardware (i.e. the initial thread). The portable numerical identifier of the logical location of task’s data is called the Software Topology Address (STA).

Figure 5(b) shows an example coarsened linear mapping (e.g. Morton order) of an adaptive Cartesian mesh such as 5(a), where each color represents a location (e.g. physical core). The advantage of this initial mapping is that it attempts to preserve inter and intra-task data reuse as the tasks that share a coarse key or close enough keys should be mapped to the same/nearby hardware locations. For algebraic representations such as matrices that arise from the discretization of Partial Differential Equations (PDEs), we use the indices of the corresponding matrix blocks to create an address. The locality notion in these can be trickier as the indices of the matrix elements do not directly express topology, however, tasks that operate on the same matrix block are still guaranteed

to share the same mapping. In the absence of topology, the STA is assigned to the nodes based on their relative location in the DAG (i.e. the depth of the node, and the location in the breadth). This is because it is known that nodes that are close in the DAG are much more likely to have data reuse. In this case, however, the DAG should exist a-priori to auto assign the STAs based on the depth and breadth of the nodes depicted by the final DAG structure. There is no such restriction for physical domains with inherent topology structure as the STA assignment in such domains is independent of the DAG structure, so dependencies can be inserted at execution time. Equations 1 to 4 show the formulas used to assign an initial location to a task based on its topology information, which is done in 4 stages.

**Stage 1: Configuring the granularity of the STA key:** since the STA is used later in this paper to index the performance model, a granularity control of how many models to create need to be available. Hence, to reduce the overhead of creating many models,  $max\_bits$  is tunable parameter, which is the maximum number of bits used to express the STA. Based on Equation 1, we allow 4 times as much as there are fine-grain resource partitions (e.g. cores in the simple case). Sensitivity analysis of the granularity of STA creation is left to a future study. Note that a “worker” refers to a logical thread.

$$max\_bits = \log_2(4 \times |workers|) \quad (1)$$

**Stage 2: Obtaining the key from topology:** in this stage depicted by Equation 2, we retrieve the space filling order ( $sfo$ ) as an integer identifier for the model using the logical location of the task’s data (e.g. Cartesian coordinates) or the location of node in the DAG if the former does not exist.

$$STA = get\_sfo\_order(logical\_loc, max\_bits) \quad (2)$$

**Stage 3: Obtaining the relative hardware location of the key:** as shown in Equation 3, this is obtained by dividing the STA by the maximum integer that can be represented using the defined granularity in Equation 1.

$$relative\_loc = \frac{STA}{2^{max\_bits}} \quad (3)$$

**Stage 4: Mapping the key to initial physical location:** in the last step (Equation 4), we map the relative location to a worker id, which falls in a moldable resource partition as shown in Figure 4. The logical worker id maps to a physical location as we explain in Section 3.2

$$worker\_id = \lfloor relative\_loc \times |workers| \rfloor \quad (4)$$

### 3.2 The Moldable Resource Partitioning

In the case of single-threaded execution, the partition id calculated by Equation 4 is the logical id of the smallest unit of execution exposed by the runtime environment, which is typically a hardware thread. However, to unleash the aforementioned potential of moldability, we express the system as a set of execution places. The system in Figure 4 shows an example hardware configured with 2 places with  $W = 4$ , 4 places with  $W = 2$  and 8 places with  $W = 1$ . A place encompasses the cores that share a resource (e.g.,

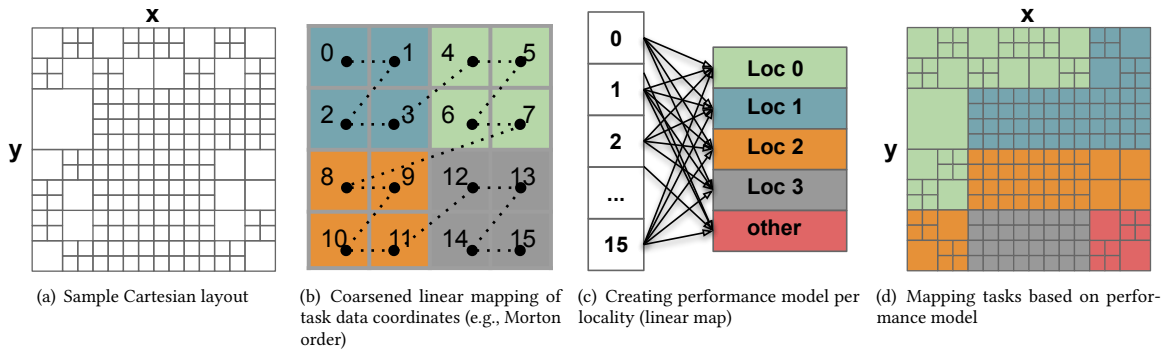


Figure 5: Overview of ARMS

Table 2: Example of the layout description

Line#	Content	Note
1	0,2,4,8,1,3,5,7	Thread affinity mappings
2	1,2,4	Widths for Leader thread 0
3	1	Widths for Leader thread 1
4	1,2	Widths for Leader thread 2
5	1	Widths for Leader thread 3
6-9	...	...

cache level, memory subsystem, network element). Thus, the relative location resembled by the line segments below Figure 4 and indicated by Equation 3 points to a moldable resource partition (initially,  $W = 1$  is selected). To allow the flexible allocation of resources, the scheduler optionally accepts a layout description file at initialization phase. For example, the dual-socket 4-core system shown in Figure 4 can be described using the file whose content is highlighted in Table 2. Line#1 of Table 2 represents the thread affinities (hardware thread id) for each of the logical threads (workers). So in this case, the runtime is configured with 8 workers, which are mapped to the listed hardware thread ids. For example worker 0 is mapped to thread id 0, worker 1 is mapped to 2 and so on. In the following 8 lines, the supported resource widths for each of the workers is specified. Hence, for leader worker 0, the supported widths are 1, 2 (spanning workers 0 and 1), and 4 (spanning workers 0 - 3). This flexible specification can easily support heterogeneous architectures, however, the evaluation of ARMS on such platforms is currently work in progress. Note that there exist tools such as hwloc [11] that can realize the system layout, and thus can be used here to generate the layout description.

**3.2.1 Moldable work-stealing.** Since ARMS is based on work-stealing, we present Figure 6 to show the interaction between work-stealing and work-sharing queues for moldable task execution. Each worker thread has a work-stealing and a work-sharing queue. The work-stealing queue includes the tasks that either are initially assigned the thread (i.e. the STA mapped thread), or the tasks that are stolen to achieve a load-balanced execution (work-balancing modes are covered in Sections 3.3.1 and 3.3.2). In Figure 6, T3 reaches the front of the queue. At this stage, the width is decided using the ARMS

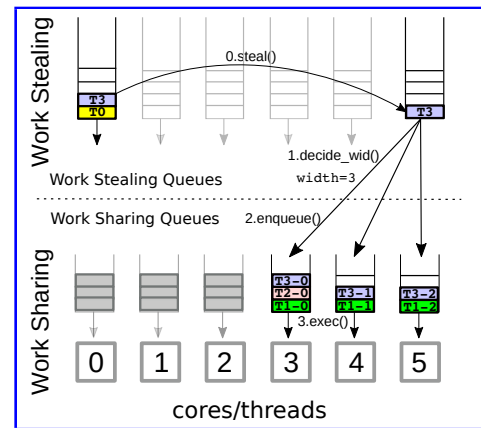


Figure 6: Moldable work-stealing scheduler

performance model, then the task is inserted to the work-sharing queues of the execution place. The queues are based on a lock-free implementation adopted from [41]. So T3 is assigned to the partition  $R = [LR = 3, W = 3]$  which represents the partitions (T3-0, T3-1, T3-2). These are executed asynchronously on workers (3,4,5). The task work function is entitled to implementing the internal scheduling scheme (similar to the OpenMP parallel regions). Hence, each task receives a partition id in the range  $[0,width-1]$ , and has access to  $R$ . In this paper, we adopt a static scheduling scheme to preserve thread-level data reuse across dependent tasks. This is semantically similar to OpenMP's static schedule for loop-parallel codes.

### 3.3 The Online Performance Model

**Identifying the model:** A key contribution of this work is defining the parameters that constitute a locality-adaptive performance model for a task. Without STA as a key (Figures 5(a) and 5(b)), the interpretation of a model would neglect the effect of data locations. Since the STA implies the mapping of task's data to a hardware location, it facilitates creating a performance model per locality for a specific task. This is to study the effects of preserving data locality for that task. Once it is initialized (e.g. using NUMA first touch policy or hwloc-lib's explicit memory pinning) in a resource partition

**Algorithm 1:** ARMS work and resource selection

---

```

1 while active do
2   if !local_queue.empty() then
3     task = pop_local_queue();
4     partitions = inclusive_partitions[local_th_id];
5     res_part = min_cost_part(task.type, task.sta,
6       partitions);
7     time = exec(task, res_part);
8     cost = time.leader x res_part.width;
9     update_cost_part(task.type, task.sta, res_part);
10  else if !inc_part_queues.empty() then
11    task = pop_one_inc_queue();
12    go to 4;
13  else if !non_inc_part_queues.empty() then
14    if stealing_attempts > THRESHOLD then
15      task = pop_non_inc_rand_queue();
16      go to 4;
17    else
18      task = peak_non_inc_rand_queue();
19      partitions = get_all_partitions();
20      res_part = min_part_cost(task.type, task.sta,
21        partitions);
22      if local_th_id in res_part then
23        task = pop_non_inc_rand_queue();
24        go to 6;
25      end
26    end
27  end
28 end

```

---

$R_i = [LR = j, W = 1]$ , the model studies the effect of molding the task and its dependencies that have the same work function. In our implementation, we express tasks as object-oriented classes for easier C++ type resolution using `std::type_id` at runtime. Alternatively, a distinct integer for each task's work function can be used for non Object-Oriented specifications. Adding the STA enables to model the performance per locality on the available system partitions. This manifests as a 2D array structure (`model[type_index][sta]`). A reference to the performance table is assigned to each task at initialization phase. For each model (Figure 5(c)), the following schemes are studied:

- The locality scheme: for the thread's local tasks, schedule within the set of inclusive partitions of the initial thread, i.e., all the partitions that share a resource with the initial task's thread as depicted by the layout description. For locality sensitive tasks, a cost-efficient place can belong to this set.
- The work-balancing scheme: use if thread's local queue is empty.

**The used performance modeling scheme:** We adopt an online history-based scheme similar to that used by StarPU [5] task programming library. We extend it to model the performance on execution places. This renders it powerful in accurately predicting the performance of fine-grain tasks, which are typical since one

of the important purposes of fine-grain task-parallelism is maximizing concurrency by creating many tasks (Task Count  $\gg$  Execution Places). Therefore, the history-based scheme proves to be effective as we show in Section 5. However, the implementation of the performance model is decoupled from the scheduler. Thus, models such as regression based or analytical models can be seamlessly used in ARMS. We start by training the model on the available places as the number of tasks that share a task is much larger than the available places (a simple recursive task parallel code like SparseLU on 64x64 blocks results in 12k tasks  $\gg$  partitions). The online history-based scheme assumes that performance is insensitive to the DAG iteration number, so a previous iteration's value can be used to predict the current iteration. However, the dynamic changes in performance can be detected as the timing values are continuously updated for the selected execution places as we show in Section 3.3.1. Eventually, for the model to result in an efficient mapping (Figure 5(d)) the locality and the work-balance schemes are used as shown in Sections 3.3.1 and 3.3.2.

**On the runtime overhead of the training scheme:** The initial STA mapping determines the distribution of the tasks over the worker threads. This offers a way to balance the work since the STA identifiers are spread over the input domain. For example, the space-filling order mapping is traditionally used to evenly partition domains with known input coordinates. Also, the even distribution is also achieved when STAs are automatically assigned by the runtime. The STAs are then normalized to the available threads as we show in Section 3.1. This reduces the penalty of under-utilization due to imbalanced partitioning.

In the case of the history-based model adopted here, the timetable is greedily filled in increasing order of the resource width (i.e. starting the execution from  $W = 1$ ). The locality scheme highlighted in Section 3.3.1 guarantees that the initial thread is always included in the subsequent schedules of the task ( $W \geq 1$ ), which ensures producer-consumer data reuse between dependent tasks. We note that, since we use an online approach, we do not separate the training phase from the actual execution of the application; all work contributes to training, which does not have the overhead imposed by offline schemes. Based on our profiles, the impact of timetable filling and the sub-optimal resource width choices is negligible as we start from the assumption that Task Count  $\gg$  Execution Places, which is valid across all experiments in Section 5. Nonetheless, if this assumption does not hold (e.g. in the case of relatively many execution places), the layout description (e.g. Table 2) can be adjusted such that the requested partitions do not span beyond the resources needed by the task with the max working set.

**3.3.1 The locality scheme.** The purpose of this scheme is to adjust the resource width within the inclusive sharing partitions. As mentioned before, a moldable task involves a work-sharing region that execute on a resource partition constituting one or multiple workers executing asynchronously. Table 3 shows the local partitions spanning threads 0 - 3 of the system shown in Figure 4. This means that logical thread 0 is included in the local resource partitions ( $LR = 0, W = 1$ ), ( $LR = 0, W = 2$ ), and ( $LR = 0, W = 4$ ). When a task is initialized in a given thread (as per the STA), the modeled performance (i.e. execution time herein) of the inclusive partitions (e.g. Table 3) is fetched. This serves as a lookup table for the indices

**Table 3: Modeled inclusive partitions**

Init thread	Local inclusive partitions
0	{[0, 1], [0, 2], [0, 4]}
1	{[1, 1], [0, 2], [0, 4]}
2	{[2, 1], [2, 2], [0, 4]}
3	{[3, 1], [2, 2], [0, 4]}

of the local partitions of each thread. It is initialized at startup given a layout description file such as Table 2. Hence, to predict the effect of moldability (i.e. changing the resource width), the partition that minimizes the cost function  $f(LR = j, W = w) = T(j) \times w$  is selected for scheduling. This cost is depicted by the cpu time perceived by the leader thread ( $T(LR)$ ) multiplied by the resource width ( $W$ ). Therefore, the higher the parallel cost, the lower the selected width and vice versa. The new cost is updated as per the new cost (Line 8). Eventually, for a latency-bound workloads, the model picks the width that matches the task’s working set size and minimizes the resource over-subscription. Also, in the events of lower DAG parallelism (at coarsening phases), the parallel cost will be lower, since more workers are available to execute the task. This results in the task being dynamically mapped to a local partition of width  $w$  that increases utilization. Algorithm 1 (Lines 3 - 8) highlights the locality scheme of ARMS.

**3.3.2 The work-balancing scheme.** Work-imbalance in dynamically scheduled DAGs is a well-studied problem, and it is especially considered in task-based runtime systems. One of the known solutions is treating the side effect of imbalance (i.e. idleness) using distributed work-stealing. In this approach, each worker thread has its own local queue that can be stolen from in events of idleness based on non-deterministic/random decisions [29, 35] or deterministic decisions [39]. ARMS uses distributed work-stealing queues. However, the stealing decisions are not entirely random. ARMS follows a heuristic method to try to maximize locality, based on the steps below:

- Local work-stealing (Algorithm 1 (Lines 10 - 11)): this is done by checking the queues of the threads of inclusive partitions. For example, if thread id 3 is idle, then based on Table 3, the inclusive threads are 0, 1, 2. The queues of these candidates are checked in round-robin fashion starting from the  $(thread\_id + 1) \% inc\_set\_size$ <sup>1</sup>. When a task is found, similar cost analysis to the locality scheme is applied.
- Non-local work-stealing (Algorithm 1 (Lines 12 - 23)): if no work is found from previous step, a random non-local task is fetched. The resource partition that globally minimizes the cost is fetched (Lines 18 - 19). The stealing thread checks if it falls in the partition of the global minimum, otherwise, the stealing attempt is rejected (i.e. when condition in Line 20 evaluates to false). When the attempts reach certain threshold, the request will be fulfilled anyway (Line 13).

<sup>1</sup>This step is dropped from Algorithm 1 for brevity

## 4 METHODOLOGY

This section describes the experimental methodology used to evaluate the contributions of this works. ARMS is integrated into `Runtime_X` [1], a DAG runtime system implemented on top of modern C++ threading extensions ( $\geq c++11$ ). `Runtime_X` is designed to flexibly evaluate scheduling policies and already features moldable tasks. However, ARMS is decoupled from the runtime internals.

### 4.1 Platforms

Experiments are performed on an Intel Skylake (Intel Xeon Gold 6130), which is a modern multicore architecture with the memory hierarchy described in Table 4. The nodes are hosted at Tetralith (NSC’s largest HPC cluster), which consists of 1908 compute nodes each with a dual socket 16-core Intel SkylakeCPU, giving a total of 61056 CPU cores. `Runtime_X` is configured to run with 32 worker threads

**The layout description file:** worker threads are mapped to the physical cores of the platform totaling 32 cores. The configured resource widths are 1, 2, 4 and 16. This means that we do not map a task across the 2 sockets. Note that there is no restriction on mapping a task to two sockets. Based on our traces, the scheduler will directly identify this as a suboptimal choice due to the cost of NUMA misses resulting from accesses from remote workers. This reflects as a high modeled parallel cost. From a memory perspective, a task can leverage (1, 2, 4, 16) x L1/L2 caches and the L3 cache, with width 16.

### 4.2 Baseline Schedulers

Below we describe and justify the baseline schedulers used:

**Random Work-Stealing Scheduler (RWS):** it is based on distributed work-stealing, where each worker greedily tries to reduce idleness by fetching work from victim queues. It has been formally introduced in [9] and has appeared in several parallel task-based libraries such as Cilk [8], and Intel TBB [28].

**Almost Deterministic Work Stealing (ADWS):** this scheduler is introduced in [38]. It is currently the state-of-the-art in work-balanced locality-aware scheduling developed as an extension to the scheduler of the MassiveThreads library [33]. It follows a deterministic task allocation based on programmer workload hints, where the work is recursively split across the DAG nodes (spawned and continuation tasks). Each worker maintains a local and a migration queue, and work stealing is only allowed inside the “work groups”. A port of ADWS has been implemented in `Runtime_X`.

**ARMS-1:** We also evaluate the proposed scheduler using 1:1 task mapping. Partition widths are persistently set to 1. Tasks are initialized and executed in the NUMA node mapped by their STA. Local stealing is preferred, then global stealing requests are fulfilled when the stealing thread reaches idleness threshold and the steal that reduces the cost function (as per the model) is chosen.

**ARMS-M:** The proposed scheduler with all components from Section 3, using 1:M task mapping. The scheduler is configured with the parameters shown in Table 5:

### 4.3 Synthetic Benchmark

To validate the adaptive online performance model adopted by ARMS, we use a synthetic DAG benchmark as shown by Figure 7.

**Table 4: Hardware structure of the used machines. Surrounded by parenthesis is the number of hardware threads that share memory/cache.**

Architecture	Sockets	Cores/socket	Threads/core	Memory(GB)	L3(MB)	L2(KB)	L1d(KB)
Intel Skylake [25]	2	16	1	48(16)	22(16)	1024(1)	32(1)

**Table 5: The configuration parameters to enable ARMS in Runtime\_X**

Option	Value	Usage
sta	enabled	capture/assign sta values
perf-model	enabled	build online perf model
idle-tries	10	idle iterations before stealing
local-steal	enabled	use local balancing scheme
global-steal	enabled	use non-local balancing scheme
moldblity	enabled	map a task to M workers

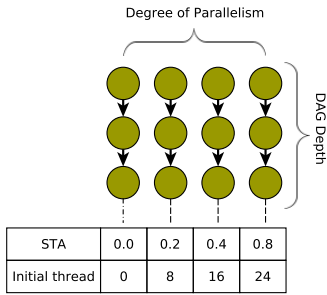


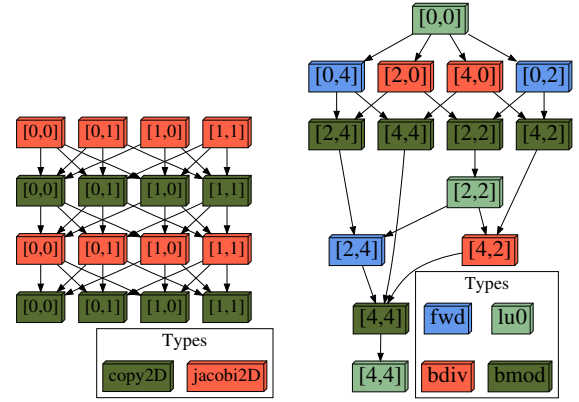
**Figure 7: The synthetic benchmark used to evaluate ARMS. This example assumes 32 threads. Number of Tasks = Parallelism × Depth**

The degree of DAG parallelism as well as the depth of the DAG are control parameters. This is useful to fix the number of tasks and understand the trade-off between parallelism and locality. Also, the tasks can be configured to be either matrix multiplication (MatMul) or Stream Triad tasks. For each chain, the table underneath Figure 7 shows the relative STA location of the thread obtained from Eq 3. The initial thread is acquired using Eq 4 with the 32 worker threads available in the experimental platform.

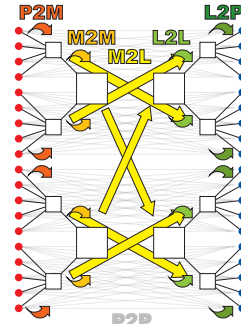
### 4.4 Applications

**Iterative DAG - HEAT:** we leverage a DAG implementation to compute heat diffusion on a 2D grid. One of the iterative numerical methods to achieve this is to use 2D Jacobi stencil. We use a 5-point stencil and create dependencies between the neighbor nodes (see Figure 8(a)). The approach involves computing the stencil in a compute task, and copying out the update in a copy task. The DAG is iteratively executed for a fixed number of 2k iterations. *For STA specification, we use the coordinates of block of mesh points involved in a task.*

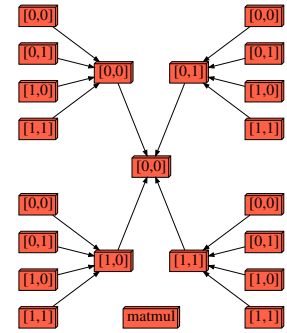
**Recursive DAG - SparseLU:** we port a SparseLU benchmark from the Barcelona OpenMP Tasks Suite [21]. This benchmark computes



(a) Stencil 2D DAG with timesteps = 2 (b) SparseLU DAG for 4x4 blocks



(c) FMM DAG Overview



(d) MatMul DAG with 2 levels of Recursion

**Figure 8: Sample dependency graphs for the analyzed applications.**

an LU matrix factorization over sparse matrices. The matrix is composed of NxN blocks, each of which has a pointer to a sub-matrix of size MxM. Load-imbalance is evident due to the sparsity of the matrix. For each phase of the LU algorithm, a task is spawned for non-empty blocks (see Figure 8(b)). *For STA specification, the matrix block indices are used.*

**Recursive DAG - The Fast Multiple Method (FMM):** we port the fmm-minimal task-based implementation from the exafmm library [48] to Runtime\_X. FMM is a popular  $O(N)$  solver for the matrix vector products arising from the solution of certain boundary integral equations [2]. It is originally used to efficiently solve the quadratic N-Body problem that appears from particle/gravitational simulations (e.g. from molecular dynamics and astrophysics). This implementation is tree-based (see Figure 8(c)). We set the leaf cell size to 64 particles. *The STA in this case leverages the Cartesian*

coordinates of the underlying tree cell.

**Recursive DAG - MatMul:** this is a cache-oblivious divide-and-conquer [22] implementation of the dense matrix multiplication. It is favorable to task-parallelism since the recursive subdivision to smaller blocks can be assigned to tasks with respective dependencies (see Figure 8(d)). The block size for the smallest block has been set to 128-256 across all experiments. *The STA is the block indices per each level of the recursion tree.*

## 5 EVALUATION

In this section, we evaluate the model's performance to assess whether it is successful in adapting the granted resources to the task's and DAG's requirements. We share the obtained empirical results comparing ARMS to the baseline schedulers. Then, we analyze the achieved performance gains by showing the schedule map for ARMS pertaining to a specific task type and location, and how locality is preserved adaptively. Also, we explain the gains by relating them to the proportion of the cumulative work time to the overall scheduling time.

### 5.1 The Adaptive Resource-Moldable Selection

We refer back to the highlighted motivational example discussed in Section 1.1 discussed in Figure 2, where we see that locality maximizing using a single threaded task may result in a sub-optimal schedule. Not only ARMS is able to place the dependencies on an efficient target NUMA node, but it is also able to maximize cache utilization by the online tuning of the resource width to match the task's requirement. Therefore, we evaluate whether the scheduler is able to adaptively tune locality depending on the initial location and size of the task's data.

In this experiment, we create a chain of task dependencies exhibiting streaming behavior as shown in Figure 7. The DAG is composed of as many chains as there are NUMA domains (i.e. 2 chains in this experiment) and each performance model is referenced by its STA. As a simplification, each model reflects the tasks whose data belong to a distinct NUMA node. Each chain's head task and data are initially pinned to a NUMA domain. Figure 10 displays the schedule trace for a single chain of 1000 tasks. The X-axis is the resource width, the Y-axis is the thread, and the Z-axis is the frequency of selection. To simplify the Y-axis, we label the NUMA node id that encloses the set of 16 threads in the id range. Also, we color the node where the task is initialized in green.

**Memory-Intensive Schedule Map:** in Figure 10(a), we expect that the dependent tasks will be scheduled to fit in the private L1 cache of the STA-mapped thread ( $R = [LR = 31, W = 1]$ ). Also, we expect that since the tasks are latency-bound, the scheduler should decide most of the time to preserve the locality. Using Algorithm 1, this is evident in more than 90% of the scheduling decisions. The second to highest frequency is observed for  $R = [LR = 30, W = 2]$ , which is still reasonable as the data size is exactly at the limit of the L1 cache. To test the automatic resource adaptation capability, we increase the problem size such that it does not fit in the private L2 cache ( $\geq 1024\text{Kb}$ ) as shown Figure 10(b). In this case, the scheduler opts for selecting the entire NUMA node (colored in green) to utilize the L3 cache totalling 22 MB ( $R = [LR = 16, W = 16]$ ), while maximizing locality at the NUMA level.

**Table 6: The resource width percentage choice as the DAG parallelism changes for a compute-intensive chain of tasks identified by an STA**

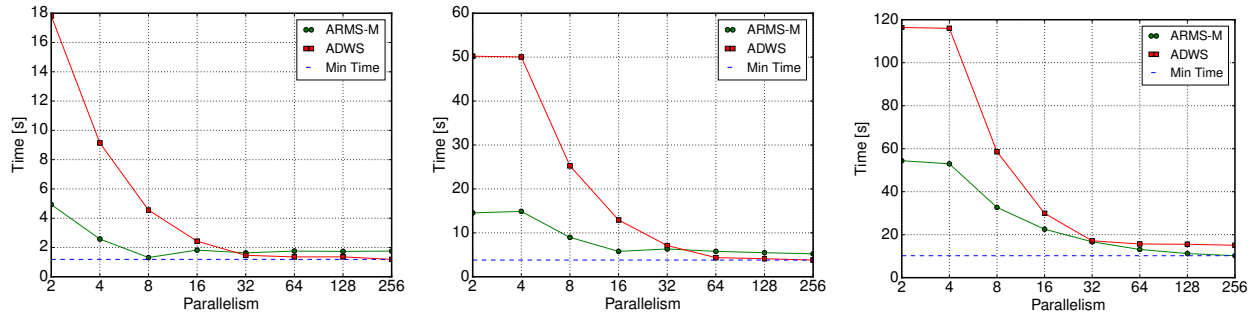
The DAG Parallelism								
Wid	2	4	8	16	32	64	128	256
1	0.1	0.3	0.5	1	1.9	65.8	96.1	95.4
2	0.1	0.2	0.3	97.8	94.2	29	1.3	0.7
4	0.1	99	98.9	0.6	1.3	3.9	0.6	0.7
8	99.7	0.4	0.5	0.6	2.6	1.3	1.9	3.3

**Compute-Intensive Schedule Map:** we also check how ARMS adjusts the schedule up to the compute/resource requirements of a chain of compute-heavy tasks which constitute a single-precision direct  $N$ -Body code [40]. In the small case shown by Figure 10(c), where tasks exceed the private L1 cache size ( $2 \times L1$ ), the scheduler conservatively picks the locality maximizing places with width ( $W = 1, 2$ ). However, the chain of large tasks (Figure 10(d)), is spread within (green region) and outside (red region) of the NUMA node containing the data, and the largest available resource widths ( $W = 8, 16$ ) are chosen to maximize floating point capability.

### 5.2 Parallelism vs Locality under ARMS

One of the important properties to study with respect to dynamic locality-aware scheduling is how the scheduler balances the trade-off between locality and parallelism, which is a known challenge in scheduling task-based programs. This is because of the fact that increasing the number of threads decreases the apparent spatial locality since access streams from independent cores are interleaved [26]. Since ARMS addresses this trade-off by adjusting the task's resource width, we analyze how it reacts to a wide range of DAG parallelisms spanning (2 - 256). The change in the DAG parallelism is highly evident in divide-and-conquer computations (a special case of fully-strict computations [9]) as we go up the recursion tree, where parallelism gets lower. Also, the DAG parallelism changes due to factors such as load-imbalance, dependency checking, synchronization and so on.

**Impact of Changing the DAG Parallelism:** to simplify the analysis, we see how ARMS behaves with different DAG parallelisms using the synthetic benchmark depicted by Figure 7. We fix the number of tasks to 50k, so that we are able to monitor the changes in performance as a function of the DAG parallelism as shown in Figure 9, with  $N=128$  for the MatMul case and  $N=512$  for the Stream Copy case. Then, we compare to ADWS as a representative of locality-aware schemes. For the challenging case of lower parallelisms (2 - 8), ARMS outperforms ADWS by approximately (3.5 $\times$ , 3 $\times$ , 2.5 $\times$ ) in the compute and memory-intensive cases shown in Figures 9(a) and 9(b), respectively. However, the gap is closed as the machine hardware parallelism is reached, with a slight degradation for higher parallel slackness than 32. This shows that ARMS has a sustainable behavior across different parallelisms and is able to effectively adapt to the case when locality preserving is not enough to achieve higher throughput. Since scheduling decisions are made on



(a) Parallel chains of Compute Intensive Matmul Tasks - Number of Tasks = 50k. N = 128 per task (b) Parallel chains of Memory Intensive Triad Tasks - Number of Tasks = 50k. N = 512 per task (c) Parallel chains of mix of Triad and Compute Tasks - Number of Tasks = 25k Triad and 25k Matmul tasks. N = 512 per task

Figure 9: ARMS performance at different DAG parallelisms.

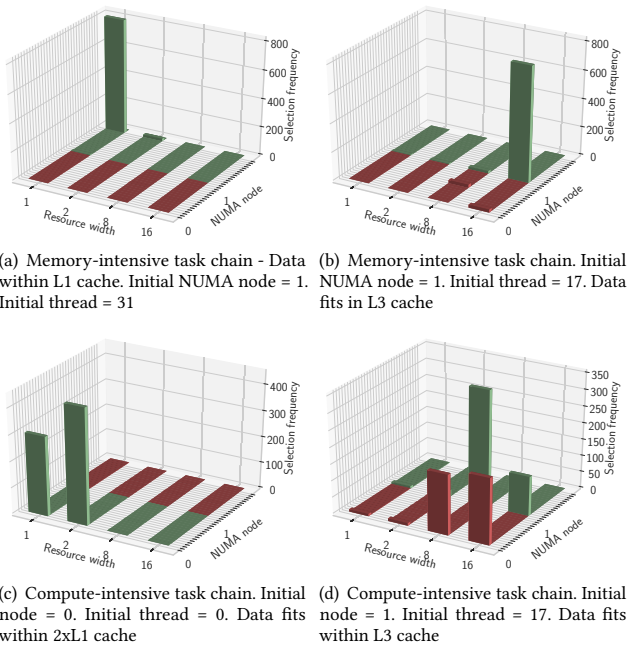


Figure 10: Resource selection model's behavior on Intel Skylake for a chain of tasks .

a per-task basis following the depicted online performance model, the aggregate effect on performance of mixing Copy and MatMul tasks combines the trends from the individual cases as shown by Figure 9(c).

**Analyzing ARMS's Performance Gain:** to demonstrate the sources of the gain, Table 6 prints the trace for the resource width choice of a single chain of MatMul task (N=128) across different runs that differ by the DAG parallelism. Since ARMS minimizes the parallel cost ( $T(P) \times w$ ), it is able to dynamically aggregate resources (i.e. increase the width) to the task at a lower DAG parallelism. For example, ARMS detects that the parallel cost of using 8 threads is lower when the DAG parallelism is 2 in 99.7% of the cases. Note

that the leader thread of this task has an id of 8 as depicted by the STA. A step-wise increase in the task resource width occurs until the DAG parallelism is 32 which matches the machine's parallelism. Beyond this point, the automatic width choice is 1. In the following sections, we study and analyze the effectiveness of these techniques in the context of different classes of applications.

### 5.3 Application Performance Evaluation

In this section, we evaluate the performance of ARMS against the baselines schedulers using various application DAGs. The applications and baselines have been described in Section 4. We also assess the impact of moldability on ARMS by studying the two scheduling variants : ARMS-M and ARMS-1. This evaluation intends to showcase the consistent enhancement that ARMS exhibits across different application classes. The granularity of the task creation across all benchmarks have been configured to be in the range of (2 - 4) L1 caches (64Kb - 256Kb) and within a private L2 cache (< 2048Kb). The initial resource width is set to 1 for all tasks (1-to-1 assignment).

**2D-Stencil:** this DAG consists of a copy task and a 5-point stencil compute grid task (Figure 8(a)) iterating 2000 times. Experiments incrementally double the mesh resolution. This application has a clear data reuse pattern across the iterations, however, the data does not fit within a single L1 cache, so moldability has a consistent improvement from 1.5x - 2x over the best baseline (ADWS) as shown by Figure 11(a). Based on our traces, ARMS molds to 2 cores in more than 90% of the scheduling decisions of the stencil compute tasks. The improvement also maps to up to an order of magnitude reduction in the application's L2 misses (Figure 12(a)).

**MatMul and SparseLU:** in the case of MatMul, the improvement takes place at a relatively larger matrix size. Since we set the leaf block size to 128, the first two cases result in 3 - 4 subdivisions, which is not enough to train the model. However, ARMS still performs better than RWS and ADWS from a matrix size of 2048 (Figures 11(b) and 12(b)). Similar improvement, shown in Figure 11(d), are achieved in SparseLU with 64x64 blocks.

**FMM:** Last but not least, considering a highly irregular DAG structure like the FMM's DAG (Figure 8(c)), ARMS-M, ARMS-1 and ADWS behave like locality-aware work-stealing schedulers due to the high

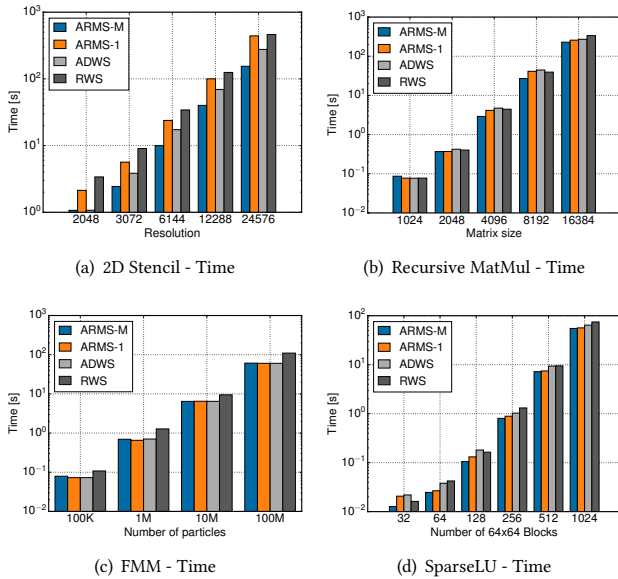


**Figure 11: Performance comparisons for task-based applications**

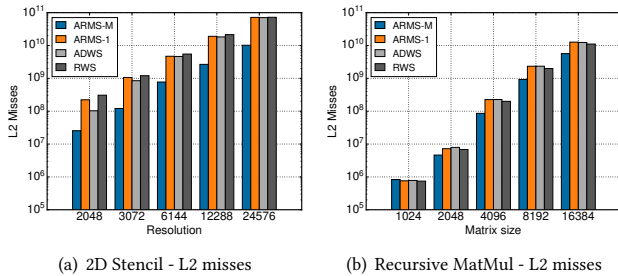


**Figure 12: L2 misses mapped to the performance gains that ARMS achieves in the 2D Stencil and Recursive MatMul applications.**

parallelism and compute intensity of FMM kernels as we can observe from Figure 11(c). However, this only shows that ARMS does best effort at either matching or outperforming the baselines without user-level computational hints or prior workload assumptions.

ARMS is effective in providing better or comparable schedules to the state-of-the-art. Molding a task to multiple threads in a locality aware-manner is especially profitable in applications with uniform data reuse patterns such as Stencil and recursive MatMul ( $N \geq 2048$ ) as demonstrated from the behaviors in Figure 12. However, due to constructing locality-adaptive performance model, ARMS-M behaves like non-moldable locality-aware schedulers (ARMS-1 and ADWS) in FMM and SparseLU. ARMS-M automatically achieves this without needing to change the user-code or having to change the scheduling options.

## 6 RELATED WORK

There has been extensive literature addressing data locality concerns in HPC applications and systems. On the theoretical level, models that predict locality for parallel programs by means of reuse distance analysis have been discussed in [14, 16, 17]. Such models aid the programmers in understanding the memory access patterns of their codes. Additionally, data-centric programming models (e.g. Legion [6]) and language extensions (e.g. Hierarchical Place Trees (HPT) [47]) require the domain expert programmer to analyze the data access regions and express the program using their interfaces, and to make explicit assignments to execution places. Despite their effectiveness, programmer level techniques (e.g. loop tiling or hierarchical cache optimizations [27]) are known to have limited portability across platforms. Hence, high-level abstractions in data locality have received a growing attention from the HPC research community [7, 43]. These abstractions are meant to adopt existing features from parallel execution frameworks, such as the affinity partitioner and task arenas from Intel TBB (Thread Building Blocks), places and processor binding from OpenMP, topology and communication reducing in MPI (Message Passing Interface) [3, 10].

As discussed, many task-based parallel libraries embrace random work-stealing scheduling mechanisms, which are provably known to be effective in maximizing dynamic load-balancing. However, they are bound to suffer from scalability issues with memory-bound tasks. To address these, techniques have been proposed to achieve locality-aware work-stealing behavior such as the Almost Deterministic Work Stealing (ADWS) [44]. This is done via deterministic mapping of tasks to resources that is applied based on the programmer's annotation of workload size. Also, the paper discusses an approach to achieve hierarchical localized work stealing. Another technique is highlighted in Scalable Locality-aware Adaptive Work-stealing Scheduler (SLAW), which also allocates the resources based on user annotations of locality (a place index) [24]. Last but not least, XKaapi [23] is a locality-aware work stealing scheduler that supports heterogeneous data flow programming targeting both CPUs and GPUs.

While these are effective techniques in reducing the side effects of random work-stealing, none of them consider the difficulty of obtaining a static classification of applications into memory and compute intensive classes. We think that ARMS is not completely orthogonal to the literature above, as it still maximizes locality when deemed necessary by the online model. However, ARMS is not yet another locality-aware scheduler, but it rather adopts a dynamic strategy and opts for locality maximizing by understanding the behavior of a task at runtime. We believe that this strategy is only more realistic considering the evolving complexity of applications and hardware.

## 7 CONCLUSIONS

In this paper, we presented a novel scheduling strategy that dynamically tunes its locality-awareness. This is achieved without statically establishing locality-aware decisions irrespective of the underlying task's arithmetic and memory footprints, a choice that can lead to suboptimal performance. By adopting an online performance model paired with platform-independent topology information, the scheduler is able to maximize locality for the latency-intensive tasks,

and to relax it for the compute-intensive counterpart. The resource moldability feature allows to adapt the granted resources to the task's requirements and to reduce the cache misses, and achieves performance gains on a variety of application DAGs.

## REFERENCES

- [1] 2021. XiTAO. <https://github.com/CHART-Team/xitao> Accessed: 2021-02-02.
- [2] Mustafa Abuljabbar, Mohammed Al Farhan, Noha Al-Harathi, Rui Chen, Rio Yokota, Hakan Bagci, and David Keyes. 2019. Extreme Scale FMM-Accelerated Boundary Integral Equation Solver for Wave Scattering. *SIAM Journal on Scientific Computing* 41, 3 (2019), C245–C268. <https://doi.org/10.1137/18M1173599> arXiv:<https://doi.org/10.1137/18M1173599>
- [3] Mustafa Abuljabbar, George S. Markomanolis, Huda Ibeid, Rio Yokota, and David Keyes. 2017. Communication Reducing Algorithms for Distributed Hierarchical N-Body Problems with Boundary Distributions. In *High Performance Computing*, Julian M. Kunkel, Rio Yokota, Pavan Balaji, and David Keyes (Eds.). Springer International Publishing, Cham, 79–96.
- [4] Umot A. Acar, Guy E. Blelloch, and Robert D. Blumofe. 2000. The Data Locality of Work Stealing. In *Proceedings of the Twelfth Annual ACM Symposium on Parallel Algorithms and Architectures* (Bar Harbor, Maine, USA) (SPAA '00). 1–12. <https://doi.org/10.1145/341800.341801>
- [5] Cédric Augonnet, Samuel Thibault, and Raymond Namyst. 2010. Automatic Calibration of Performance Models on Heterogeneous Multicore Architectures. In *Euro-Par 2009 – Parallel Processing Workshops*, Hai-Xiang Lin, Michael Alexander, Martti Forsell, Andreas Knüpfer, Radu Prodan, Leonel Sousa, and Achim Streit (Eds.). Springer Berlin Heidelberg, Berlin, Heidelberg, 56–65.
- [6] Michael Bauer, Sean Treichler, Elliott Slaughter, and Alex Aiken. 2012. Legion: Expressing locality and independence with logical regions. In *SC '12: Proceedings of the International Conference on High Performance Computing, Networking, Storage and Analysis*. 1–11. <https://doi.org/10.1109/SC.2012.71>
- [7] Michael Bauer, Sean Treichler, Elliott Slaughter, and Alex Aiken. 2012. Legion: Expressing Locality and Independence with Logical Regions. In *Proceedings of the International Conference on High Performance Computing, Networking, Storage and Analysis* (Salt Lake City, Utah) (SC '12). IEEE Computer Society Press, Los Alamitos, CA, USA, Article 66, 11 pages. <http://dl.acm.org/citation.cfm?id=2388996.2389086>
- [8] Robert D. Blumofe, Christopher F. Joerg, Bradley C. Kuszmaul, Charles E. Leiserson, Keith H. Randall, and Yuli Zhou. 1995. Cilk: An Efficient Multithreaded Runtime System. In *Proceedings of PPOPP '95*. ACM.
- [9] Robert D. Blumofe and Charles E. Leiserson. 1999. Scheduling Multithreaded Computations by Work Stealing. *J. ACM* 46, 5 (Sept. 1999), 720–748.
- [10] George Bosilca, Aurelien Bouteiller, Anthony Danalis, Thomas Herault, Pierre Lemarinier, and Jack Dongarra. 2011. DAGuE: A Generic Distributed DAG Engine for High Performance Computing. In *Proceedings of the 2011 IEEE International Symposium on Parallel and Distributed Processing Workshops and PhD Forum (IPDPSW '11)*. IEEE Computer Society, Washington, DC, USA, 1151–1158. <https://doi.org/10.1109/IPDPS.2011.281>
- [11] Francois Broqueus, Jérôme Clet-Ortega, Stéphanie Moreaud, Nathalie Furmento, Brice Goglin, Guillaume Mercier, Samuel Thibault, and Raymond Namyst. 2010. hwloc: A Generic Framework for Managing Hardware Affinities in HPC Applications. In *2010 18th Euromicro Conference on Parallel, Distributed and Network-based Processing*. 180–186. <https://doi.org/10.1109/PDP.2010.67>
- [12] T. Burd, N. Beck, S. White, M. Paraschou, N. Kalyanasundharam, G. Donley, A. Smith, L. Hewitt, and S. Naffziger. 2019. "Zeppelin": An SoC for Multichip Architectures. *IEEE Journal of Solid-State Circuits* 54, 1 (Jan. 2019), 133–143. <https://doi.org/10.1109/JSSC.2018.2873584>
- [13] Steve Carr, Kathryn S. McKinley, and Chau-Wen Tseng. 1994. Compiler Optimizations for Improving Data Locality. In *Proceedings of the Sixth International Conference on Architectural Support for Programming Languages and Operating Systems* (San Jose, California, USA) (ASPLOS VI). Association for Computing Machinery, New York, NY, USA, 252–262. <https://doi.org/10.1145/195473.195557>
- [14] Calin Cascaval and David A. Padua. 2003. Estimating Cache Misses and Locality Using Stack Distances. In *International Conference on Supercomputing (ICS-03). Proceedings of ICS'03*.
- [15] Quan Chen, Minyi Guo, and Haibing Guan. 2014. LAWS: Locality-aware Work-stealing for Multi-socket Multi-core Architectures. In *Proceedings of the 28th ACM International Conference on Supercomputing* (Munich, Germany) (ICS '14). ACM, New York, NY, USA, 3–12. <https://doi.org/10.1145/2597652.2597665>
- [16] Chen Ding and Trishul Chilimbi. 2009. *A Composable Model for Analyzing Locality of Multi-threaded Programs*. Technical Report MSR-TR-2009-107. Microsoft Research.
- [17] Chen Ding and Yutao Zhong. 2003. Predicting Whole-Program Locality through Reuse Distance Analysis. In *Proceedings of PLDI'03*.
- [18] Andi Drebes, Karine Heydemann, Nathalie Drach, Antoniu Pop, and Albert Cohen. 2014. Topology-Aware and Dependence-Aware Scheduling and Memory Allocation for Task-Parallel Languages. *ACM Trans. Archit. Code Optim.* 11, 3, Article 30 (Aug. 2014), 25 pages. <https://doi.org/10.1145/2641764>
- [19] Andi Drebes, Antoniu Pop, Karine Heydemann, Albert Cohen, and Nathalie Drach. 2016. Scalable Task Parallelism for NUMA: A Uniform Abstraction for Coordinated Scheduling and Memory Management. In *Proceedings of the 2016 International Conference on Parallel Architectures and Compilation* (Haifa, Israel) (PACT '16). Association for Computing Machinery, New York, NY, USA, 125–137. <https://doi.org/10.1145/2967938.2967946>
- [20] Alejandro Duran, Eduard Ayguade, Rosa M. Badiá, Jesus Labarta, Lluís Martinell, Xavier Martorell, and Judit Planas. 2011. OmpSs: A proposal for programming Heterogeneous Multi-core Architectures. *Parallel Processing Letters* 21, 02 (2011), 173–193. <https://doi.org/10.1142/S0129626411000151> arXiv:<http://www.worldscientific.com/doi/pdf/10.1142/S0129626411000151>
- [21] Alejandro Duran, Xavier Teruel, Roger Ferrer, Xavier Martorell, and Eduard Ayguade. 2009. Barcelona OpenMP Suite: A Set of Benchmarks Targeting the Exploitation of Task Parallelism in OpenMP. In *Proceedings of the 2009 International Conference on Parallel Processing (ICPP '09)*. 124–131. <https://doi.org/10.1109/ICPP.2009.64>
- [22] M. Frigo, C. E. Leiserson, H. Prokop, and S. Ramachandran. 1999. Cache-oblivious algorithms. In *40th Annual Symposium on Foundations of Computer Science (Cat. No.99CB37039)*. 285–297. <https://doi.org/10.1109/SFCS.1999.814600>
- [23] T. Gautier, J. V. F. Lima, N. Maillard, and B. Raffin. 2013. XKaapi: A Runtime System for Data-Flow Task Programming on Heterogeneous Architectures. In *IEEE 27th International Symposium on Parallel Distributed Processing (IPDPS'13)*. 1299–1308. <https://doi.org/10.1109/IPDPS.2013.66>
- [24] Yi Guo, Jisheng Zhao, Vincent Cave, and Vivek Sarkar. 2010. SLAW: a Scalable Locality-aware Adaptive Work-stealing Scheduler. In *Proceedings of IPDPS'10*.
- [25] Intel. [n.d.]. Intel® Xeon® Gold 6130. <https://ark.intel.com/content/www/us/en/ark/products/120492/intel-xeon-gold-6130-processor-22m-cache-2-10ghz.html>
- [26] M. K. Jeong, D. H. Yoon, D. Sunwoo, M. Sullivan, I. Lee, and M. Erez. 2012. Balancing DRAM locality and parallelism in shared memory CMP systems. In *IEEE International Symposium on High-Performance Comp Architecture*. 1–12. <https://doi.org/10.1109/HPCA.2012.6168944>
- [27] Markus Kowarschik and Christian Weiß. 2003. *An Overview of Cache Optimization Techniques and Cache-Aware Numerical Algorithms*. Springer Berlin Heidelberg, Berlin, Heidelberg, 213–232.
- [28] A Kukanov and M Voss. 2007. The foundations for scalable multi-core software in Intel Threading Building Blocks. *Intel Technology Journal* 11 (2007), 309–322. Issue 4. <https://doi.org/10.1535/itj.1104>
- [29] V. Kumar, K. Murthy, V. Sarkar, and Y. Zheng. 2016. Optimized Distributed Work-Stealing. In *2016 6th Workshop on Irregular Applications: Architecture and Algorithms (IA3)*. 74–77.
- [30] Zoltan Majo and Thomas R. Gross. 2011. Memory System Performance in a NUMA Multicore Multiprocessor. In *Proceedings of the 4th Annual International Conference on Systems and Storage* (Haifa, Israel) (SYSTOR '11). Association for Computing Machinery, New York, NY, USA, Article 12, 10 pages. <https://doi.org/10.1145/1987816.1987832>
- [31] David L. Mulnix. [n.d.]. Intel® Xeon® Processor Scalable Family Technical Overview. <https://software.intel.com/content/www/us/en/develop/articles/intel-xeon-processor-scalable-family-technical-overview.html>
- [32] S. Naffziger, K. Lepak, M. Paraschou, and M. Subramony. 2020. 2.2 AMD Chiplet Architecture for High-Performance Server and Desktop Products. In *2020 IEEE International Solid-State Circuits Conference - (ISSCC)*. 44–45. <https://doi.org/10.1109/ISSCC19947.2020.9063103> ISSN: 2376-8606.
- [33] Jun Nakashima and Kenjiro Taura. 2014. *MassiveThreads: A Thread Library for High Productivity Languages*. Springer Berlin Heidelberg, Berlin, Heidelberg, 222–238. [https://doi.org/10.1007/978-3-662-44471-9\\_10](https://doi.org/10.1007/978-3-662-44471-9_10)
- [34] Stephen L. Olivier, Allan K Porterfield, Kyle B Wheeler, Michael Spiegel, and Jan F Prins. 2012. OpenMP task scheduling strategies for multicore NUMA systems. *The International Journal of High Performance Computing Applications* 26, 2 (2012), 110–124. <https://doi.org/10.1177/1094342011434065> arXiv:<https://doi.org/10.1177/1094342011434065>
- [35] J. Paudel, O. Tardieu, and J. N. Amaral. 2013. On the Merits of Distributed Work-Stealing on Selective Locality-Aware Tasks. In *2013 42nd International Conference on Parallel Processing*. 100–109.
- [36] Isaac Sánchez Barrera, Miquel Moretó, Eduard Ayguadé, Jesús Labarta, Mateo Valero, and Marc Casas. 2018. Reducing Data Movement on Large Shared Memory Systems by Exploiting Computation Dependencies. In *Proceedings of the 2018 International Conference on Supercomputing* (Beijing, China) (ICS '18). Association for Computing Machinery, New York, NY, USA, 207–217. <https://doi.org/10.1145/3205289.3205310>
- [37] M. Sato, Y. Ishikawa, H. Tomita, Y. Kodama, T. Odajima, M. Tsuji, H. Yashiro, M. Aoki, N. Shida, I. Miyoshi, K. Hirai, A. Furuuya, A. Asato, K. Morita, and T. Shimizu. 2020. Co-Design for A64FX Manycore Processor and "Fugaku". In *SC20: International Conference for High Performance Computing, Networking, Storage and Analysis*. 1–15. <https://doi.org/10.1109/SC41405.2020.00051>

- [38] Shumpei Shiina and Kenjiro Taura. 2019. Almost Deterministic Work Stealing. In *Proceedings of the International Conference for High Performance Computing, Networking, Storage and Analysis* (Denver, Colorado) (SC '19). Association for Computing Machinery, New York, NY, USA, Article 47, 16 pages. <https://doi.org/10.1145/3295500.3356161>
- [39] Shumpei Shiina and Kenjiro Taura. 2019. Almost Deterministic Work Stealing. In *Proceedings of the International Conference for High Performance Computing, Networking, Storage and Analysis* (Denver, Colorado) (SC '19). Association for Computing Machinery, New York, NY, USA, Article 47, 16 pages. <https://doi.org/10.1145/3295500.3356161>
- [40] Rainer Spurzem. 1999. Direct N-body simulations. *J. Comput. Appl. Math.* 109, 1 (1999), 407–432. [https://doi.org/10.1016/S0377-0427\(99\)00166-1](https://doi.org/10.1016/S0377-0427(99)00166-1)
- [41] Herb Sutter. [n.d.]. *Writing Lock-Free Code: A Corrected Queue*. <https://www.drdobbs.com/parallel/writing-lock-free-code-a-corrected-queue/210604448>
- [42] S. Tzilis, M. Pericás, P. Trancoso, and I. Sourdis. 2017. SWAS: Stealing Work Using Approximate System-Load Information. In *2017 46th International Conference on Parallel Processing Workshops (ICPPW)*. 309–318. <https://doi.org/10.1109/ICPPW.2017.51>
- [43] D. Unat, A. Dubey, T. Hoefler, J. Shalf, M. Abraham, M. Bianco, B. L. Chamberlain, R. Cledat, H. C. Edwards, H. Finkel, K. Fuerlinger, F. Hannig, E. Jeannot, A. Kamil, J. Keasler, P. H. J. Kelly, V. Leung, H. Ltaief, N. Maruyama, C. J. Newburn, and M. Pericás. 2017. Trends in Data Locality Abstractions for HPC Systems. *IEEE Transactions on Parallel and Distributed Systems* 28, 10 (Oct 2017), 3007–3020. <https://doi.org/10.1109/TPDS.2017.2703149>
- [44] B. Vikranth, Rajeev Wankar, and C. Raghavendra Rao. 2019. Affinity-Aware Synchronization in Work Stealing Run-Times for NUMA Multi-core Processors. In *Advanced Computing and Communication Technologies*, Jyotsna Kumar Mandal, Dhananjay Bhattacharyya, and Nitin Auluck (Eds.). Springer Singapore, Singapore, 121–131.
- [45] Kyle Wheeler, Richard Murphy, and Douglas Thain. 2008. Qthreads: An API for Programming with Millions of Lightweight Threads, In *Proceedings of MTAAP '08. Proceedings of MTAAP '08*.
- [46] Thomas Willhalm and Nicolae Popovici. 2008. Putting Intel® Threading Building Blocks to Work. In *Proceedings of the 1st International Workshop on Multicore Software Engineering* (Leipzig, Germany) (IWMSE '08). Association for Computing Machinery, New York, NY, USA, 3–4. <https://doi.org/10.1145/1370082.1370085>
- [47] Yonghong Yan, Jisheng Zhao, Yi Guo, and Vivek Sarkar. 2010. Hierarchical Place Trees: A Portable Abstraction for Task Parallelism and Data Movement. In *Languages and Compilers for Parallel Computing*, Guang R. Gao, Lori L. Pollock, John Cavazos, and Xiaoming Li (Eds.). Springer Berlin Heidelberg, Berlin, Heidelberg, 172–187.
- [48] Rio Yokota et al. 2017. ExaFMM. <https://github.com/exafmm/minimal>.